Available online at www.sciencedirect.com
ScienceDirect
Journal of Power Sources 179 (2008) 504–510
JOURNAL OF POWER SOURCES
www.elsevier.com/locate/jpowsour

# Characteristics of aluminum-reinforced γ-$LiAlO_2$ matrices for molten carbonate fuel cells

Jong-Jin Lee [a], Hyun-Jong Choi [a], Sang-Hoon Hyun [a,*], Hee-Chun Im [b]

[a] *School of Advanced Materials Science and Engineering, Yonsei University, Seoul 120-749, Republic of Korea*
[b] *KEPRI, Korea Electric Power Research Institute, Daejeon 103-16, Republic of Korea*

Received 4 September 2007; received in revised form 29 November 2007; accepted 14 December 2007
Available online 11 January 2008

**Abstract**

A key component in molten carbonate fuel cells (MCFCs) is the electrolyte matrix, which provides both ionic conduction and gas sealing. During initial MCFC stack start-up and operation (650 °C), the matrix experiences both mechanical and thermal stresses as a result of the difference in thermal expansion coefficients between the $LiAlO_2$ ceramic particles and the carbonate electrolyte that causes cracking of the matrix. A pure γ-$LiAlO_2$ matrix, however, has poor mechanical strength and low thermal expansion coefficients. In this study, fine γ-$LiAlO_2$ powders and pure Al (3/20/50 μm)/$Li_2CO_3$ particles are used as a matrix and as reinforcing materials, respectively. The Al phase transforms completely into γ-$LiAlO_2$ at 650 °C within 10 h. The mechanical strength of these matrices (283.48 gf mm$^{-2}$) increases nearly threefold relative to that of a pure γ-$LiAlO_2$ matrix (104.01 gf mm$^{-2}$). The mismatch of the thermal expansion coefficient between the matrix and electrolyte phases can be controlled by adding Al particles, which results in improved thermal stability in the initial heating-up step. In unit-cell and thermal-cycling tests, the optimized matrix demonstrates superior performance over pure γ-$LiAlO_2$ matrices.


*Keywords:* Aluminum particles; γ-$LiAlO_2$ electrolyte matrix; Molten carbonate fuel cell; Thermal expansion coefficient; Mechanical strength

## 1. Introduction

Molten carbonate fuel cells (MCFCs) have attracted great interest as they are expected to be central to the most efficient MW-class power generation systems for use in the near future. Although MCFC offers many advantages, e.g., very high electrochemical conversion efficiency and safe and pollution-free operation, a substantial improvement in operating life-time is required before commercialization can be considered [1]. A key component in the MCFC is the electrolyte matrix, which provides both ionic conduction and gas sealing. γ-$LiAlO_2$ materials are typically used as the electrolyte matrix. These materials are very reactive in alkali molten carbonate electrolyte at 650 °C [2]. Hatoh et al. [3] studied the behaviour of a γ-$LiAlO_2$ matrix sintered under MCFC conditions and found that the size of the γ-$LiAlO_2$ particles remained stable at lower temperatures in molten carbonate with high Li:K ratios under a high partial pressure of carbon dioxide.

Another important property of the matrix is its mechanical strength. The electrolyte matrix has to remain substantially crack-free in order to provide effective gas-sealing properties during MCFC operation. During initial start-up and operation of a MCFC stack, the matrix experiences both mechanical and thermal stresses as a result of the difference between the thermal expansion coefficients of the $LiAlO_2$ ceramic particles and the carbonate electrolyte. This feature can cause cracking of the matrix [4]. A pure γ-$LiAlO_2$ matrix has poor mechanical strength and a low thermal expansion coefficient.

Various approaches for improving the crack resistance and extending the life of electrolyte matrices have been proposed. Alumina fibre reinforcements were used in an attempt to improve the mechanical properties of γ-$LiAlO_2$ matrices [5]. Although the fibres improved the mechanical strength, these materials decay gradually in molten carbonates at the operating temper-

* Corresponding author. Tel.: +82 2 2123 2850; fax: +82 2 365 5882.
*E-mail address:* prohsh@yonsei.ac.kr (S.-H. Hyun).

0378-7753/$ – see front matter © 2008 Elsevier B.V. All rights reserved.
doi:10.1016/j.jpowsour.2007.12.110

ature. Second-phase crack deflectors such as large γ-$LiAlO_2$ particles have been used but, to date, these materials have not promoted the desired strengthening and longevity of the matrix. Rod-shaped γ-$LiAlO_2$ particles, which are superior to fibres in terms of their chemical and thermal stability and mechanical strength have been developed as a new material for reinforcing the MCFC matrix [6,7]. Nevertheless, these materials do not yet meet the commercialization requirements of the MCFC system. Aluminum acetylacetonate has been employed as a sintering aid for the $LiAlO_2$ matrix. This material increases the growth of the necks of the matrix with sintering time and, correspondingly, the mechanical strength experiences an abrupt increase [8].

In this study, aluminum particles (which are cost-effective) together with lithium carbonate ($Li_2CO_3$) particles are applied as a reinforcement for a MCFC matrix. The characteristics of the Al-reinforced γ-$LiAlO_2$ matrix are investigated via a three-point bending test, X-ray diffraction analysis (XRD), scanning electron microscopic observations, and dilatometer and mercury porosimeter measurements. The improvement in performance of this matrix is investigated by thermal-cycling tests and nitrogen gas crossover under MCFC operating conditions.

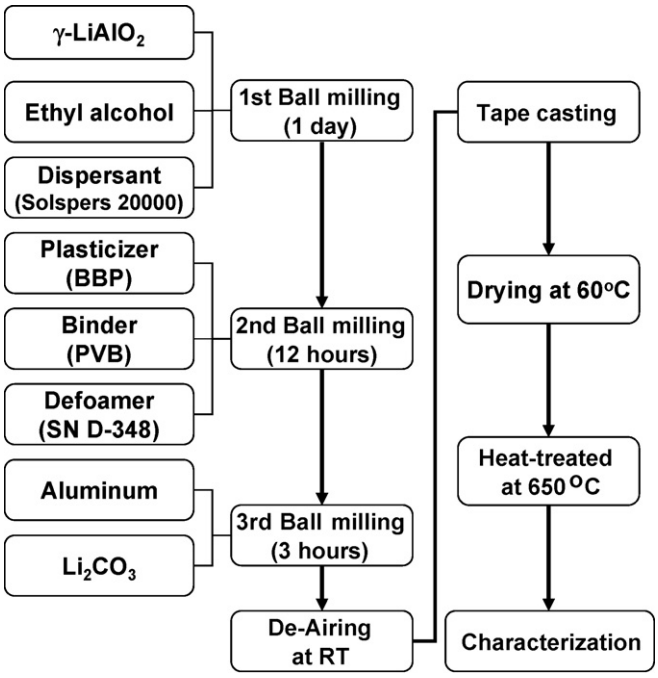


Fig. 1. Overall process flow chart.

## 2. Experimental

The MCFC matrices were fabricated by tape casting of a slurry that consisted of an organic solvent, additives, and solid constituents of commercial γ-$LiAlO_2$ particles (Cyprus Foote Mineral Co.) and Al particles (Duksan). The microstructure (e.g., morphology, porosity, pore-size distribution) and mechanical properties of the aluminum-reinforced matrices were modulated via the use of different particle sizes of aluminum powder (Kojundo 3 μm, 20 μm and Duksan 50 μm). A flow chart showing the overall experiment is presented in Fig. 1, and the experimental procedures for each step are described in detail below.

Commercial γ-$LiAlO_2$ particles for a highly porous powder were used as the solid constituent of the MCFC matrix. A dispersant medium was prepared with ethyl alcohol (99%, Duksan) instead of water due to the high reactivity of $LiAlO_2$ with water. Polyvinylbutyral (98%, Sigma Co.) was used as a binder, dibutylphthalate (99%, Junsei Co.) as a plasticizer, solsperse-20000 (Imperial Chemical Ind.) as a dispersant, and SN D-348 (San Nopco, Korea) as a defoamer. The slurry composition is given in Table 1 (note that the composition was optimized in a previous work for the reinforcement of free γ-$LiAlO_2$ matrices [9]). Non-reinforced matrices comprised of a mixture of 50 wt.% HAS-10 particles and 50 wt.% LSA-50 particles of a low surface area (0.1 $m^2\,g^{-1}$) were fabricated as a standard for comparison with the reinforced matrices. The aluminum-reinforced γ-$LiAlO_2$ matrices were prepared with aluminum of various different particle sizes (3/20/50 μm), using only HAS-10 type commercial γ-$LiAlO_2$ powders with a high specific surface area (10 $m^2\,g^{-1}$).

To determine the aluminum content that yielded the highest mechanical strength, the measured specimens were fabricated

Table 1
Slurry compositions optimized for Al-reinforced matrices

| | Material | | | | | | | |
|---|---|---|---|---|---|---|---|---|
| | Solid (wt.%) | | | Solvent (wt.%) | Binder (wt.%) | Plasticizer (wt.%) | Dispersant (wt.%) | Deformer (wt.%) |
| | γ-$LiAlO_2$ | Al | $Li_2CO_3$ | | | | | |
| Zero Al content | 38.813 | | | 38.378 | 9.68 | 11.62 | 0.755 | 0.755 |
| 5 vol.% Al content | 35.819 | 2 | 1 | | | | | |

Table 2
Conditions and characteristics of single-cell operation

| Unit cell component | Size (mm) | Thickness (mm) | Porosity (%) | Pore size (μm) | Material |
|---|---|---|---|---|---|
| Anode | 11 × 11 | 0.75 | 63.7 | 3 | Ni |
| Cathode | 10 × 10 | 0.65 | 64.1 | 7 | In situ lithiated NiO |
| Electrolyte | 13 × 13 | – | – | – | $Li_2CO_3/K_2CO_3$ mole ratio (62:38) |

using a uni-axial press. The content of the aluminum particles was varied from 0 vol.% to 30 vol.% to optimize the reinforced MCFC matrix. According to the results, it was determined that the aluminum-reinforced matrix should be fabricated by tape casting.

To evaluate the cell performance, a single cell (10 cm × 10 cm) was used. The experimental conditions and characteristics of the operation are summarized in Table 2. Two single cells were prepared, one using standard matrices and the other using aluminum-reinforced matrices. The fuel gases passing through the anode consisted of $H_2$, $CO_2$, and $H_2O$ in a 72:18:10 mole ratio; the cathode gas was air and $CO_2$ in a 70:30 mole ratio. Cell voltage was measured at open-circuit and at 150 mA $cm^{-2}$, which is the normal load. The gas composition at the anode exit was analyzed with a gas chromatograph (Hewlett-Packard 5890 series II, USA).

A green matrix sheet was heat-treated at 650 °C for 10 h. A three-point bending test was performed on the sintered sheet using a UTM (Model 1127, Instron, USA) to measure the mechanical strength. The thermal expansion coefficient was assessed using a dilatometer (DIL 402C, Netzsch, Germany) and the morphology of the aluminum-reinforced matrix was observed by scanning electronic microscopy (SEM; Model S4200, Hitachi Ltd., Japan). The pore-size distribution and porosity of the matrices were measured by means of mercury porosimetry (Model Autopore II, Micrometrics Instrument Corp., USA).

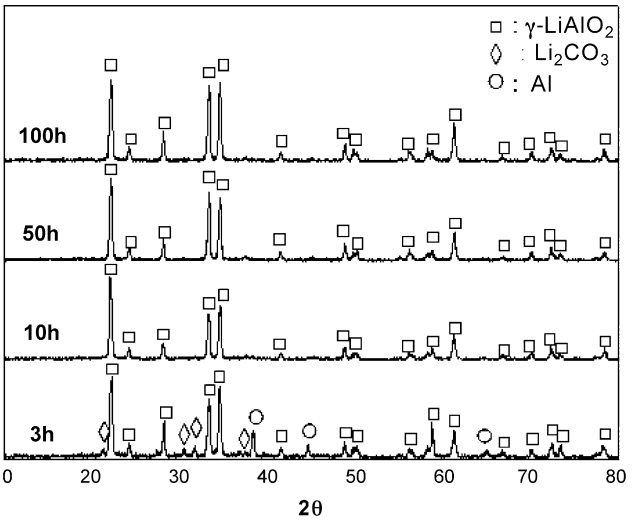


Fig. 2. X-ray diffraction patterns of γ-$LiAlO_2$ matrices reinforced by aluminum and $Li_2CO_3$ particles with heat-treatment time at 650 °C.

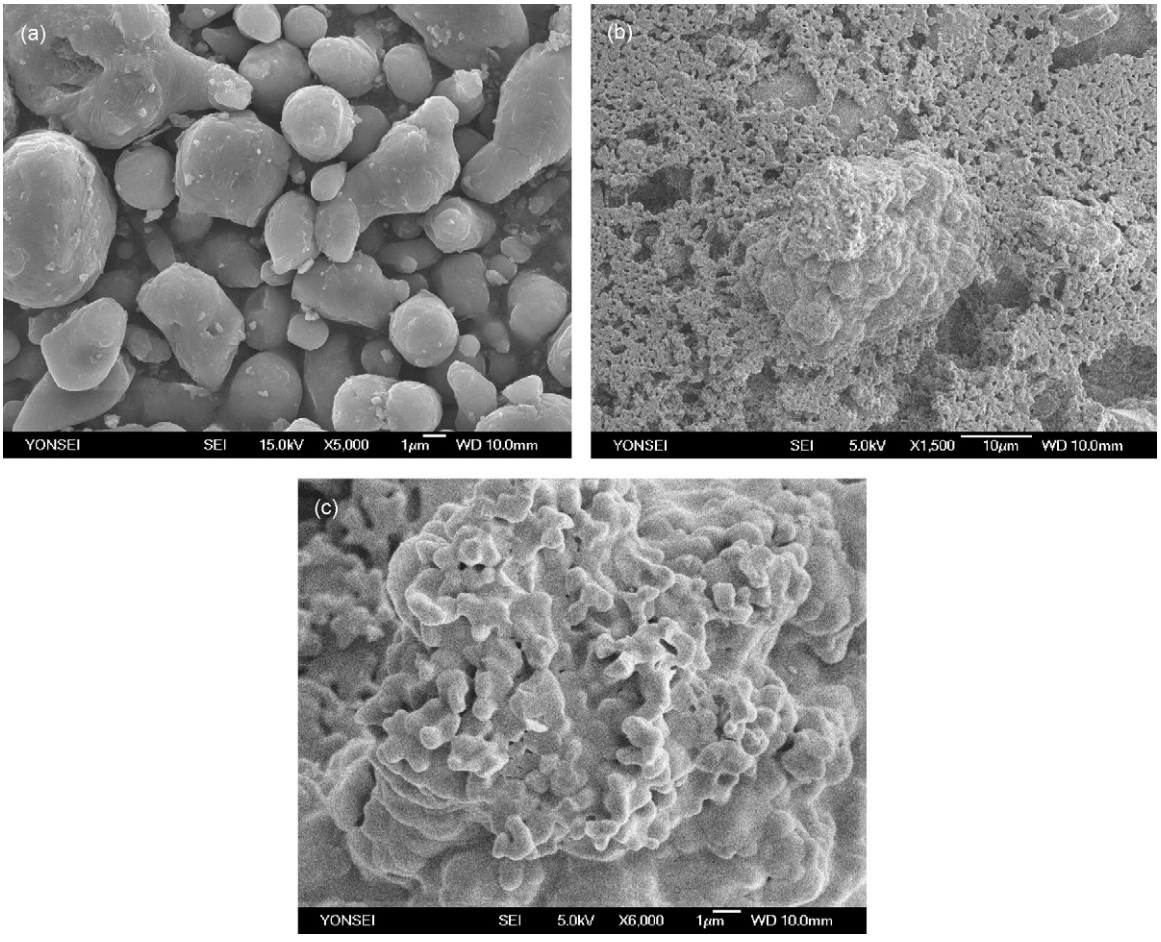


Fig. 3. Scanning electron micrographs of aluminum particles: (a) raw aluminum particle, (b) aluminum-reinforced matrix, and (c) aluminum melting and oxide phase.

## 3. Results and discussion

### 3.1. Reaction mechanism of aluminum and $Li_2CO_3$

Aluminum metal particles have a low melting point (660 °C). In addition, they are transformed into oxide phases at 650 °C according to

$$4Al + 2Li_2CO_3 + O_2 \rightarrow 2LiAlO_2 + 2CO_2 \quad (1)$$

This phenomenon is verified by the XRD patterns given in Fig. 2. It can be seen that the phases of $Li_2CO_3$ and aluminum remain unchanged during the sintering process (650 °C for 3 h). After heat-treatment at 650 °C for 10 h, all of the aluminum and $Li_2CO_3$ particles are transformed into γ-$LiAlO_2$; additional phase transformations are not observed.

Scanning electron micrographs of the morphologies of the aluminum particles before and after sintering at 650 °C are presented in Fig. 3. The raw aluminum particles have a smooth metallic surface. After sintering at 650 °C, however, the surface becomes rough, melts and transforms into an oxide phase by reacting with $Li_2CO_3$. This reaction also shows good coupling with the matrix surrounding the particles.

### 3.2. Thermal expansion coefficients of Al-reinforced matrices

The MCFC matrix experiences cracking during initial start-up due to the difference in the thermal expansion coefficients between the electrolyte materials ($\alpha = 20 \times 10^{-6}$ mm °$C^{-1}$) and γ-$LiAlO_2$ matrix ($\alpha = 10 \times 10^{-6}$ mm °$C^{-1}$). Accordingly, the matrix requires reinforcement with an additional second-phase that has a higher thermal expansion coefficient than $LiAlO_2$. Among the second-phase reinforcements, aluminum metal particles provide a very high thermal expansion coefficient ($\alpha = 23 \times 10^{-6}$ mm °$C^{-1}$) during both start-up and operation.

The dilatometry results given in Fig. 4 for the Al-reinforced specimens were measured by calibration of the linear section in a high temperature range from 300 °C to 600 °C, as compensation of the dilatometry machine and rearrangement of the materials comprising the specimen occur at a low temperature of 250 °C. The specimens were fabricated by pre-sintering at a low temperature of 400 °C and were gradually reduced in size by the measuring pressure under 200 °C. According to these calibration results, it is found that the thermal expansion coefficient of the matrix with the addition of aluminum improves as the aluminum content increases. Thus, the mismatch in the thermal expansion coefficients of the matrix and

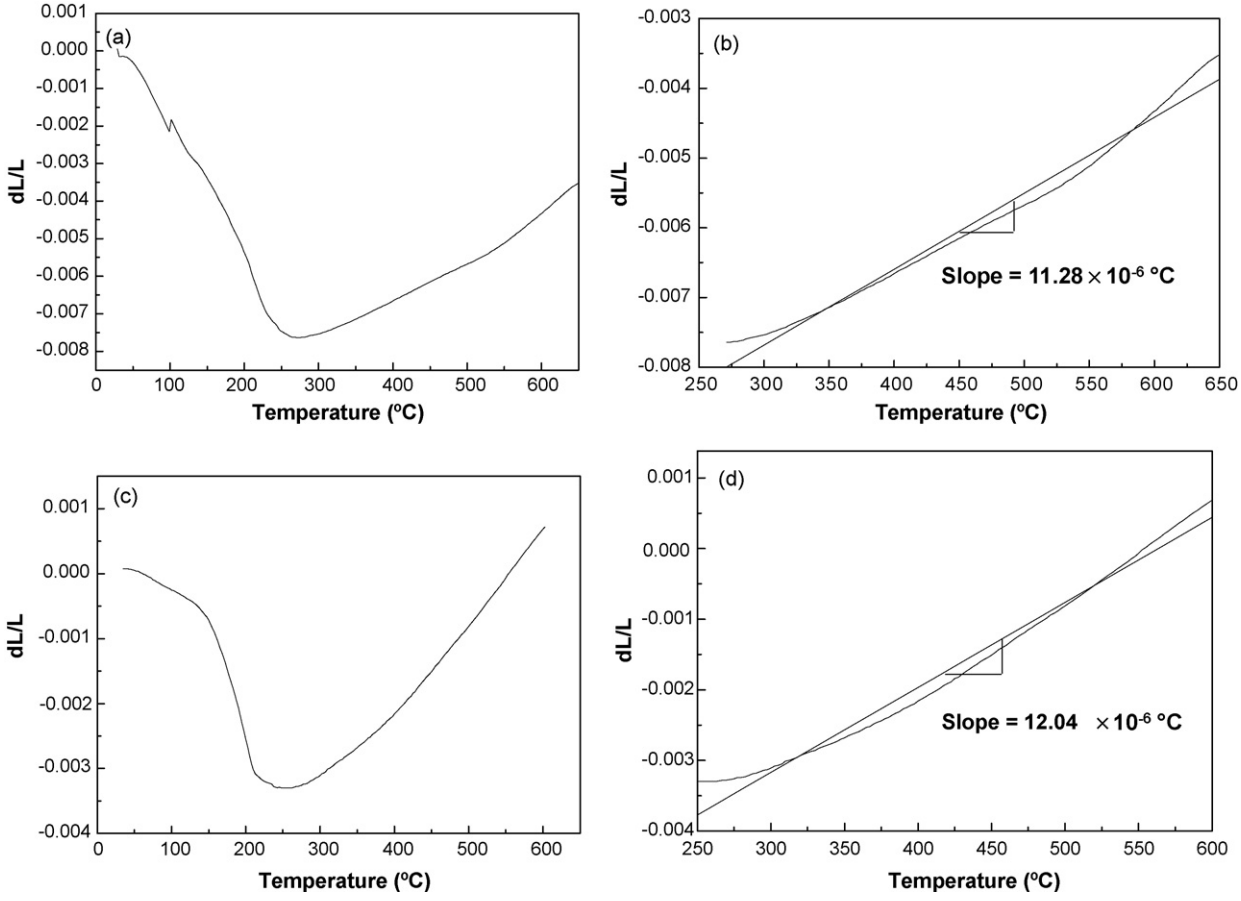


Fig. 4. Thermal expansion coefficients of γ-$LiAlO_2$ matrices: (a) raw data and (b) calculated data for aluminum particle (5 vol.%) reinforced matrix; (c) raw data, and (d) calculated data for aluminum particle (10 vol.%) reinforced matrix.

the electrolyte phases can be controlled by adding aluminum particles.

### 3.3. Mechanical strength of reinforced matrices

Particles are generally used to improve certain properties of materials or matrices, such as stiffness, behaviour with temperature, resistance to abrasion, etc. [10]. Any reinforcement in the stress field at the tip of a propagating crack perturbs the crack front causing a reduction in the stress intensity in the matrix. This of course hinders the propagation of the crack, namely crack bowing and crack deflection. Crack bowing toughening increases with the volume fraction of reinforcement and depends on the magnitude of the crack-reinforcement which, in turn, is determined by the separation and toughness of the reinforcement [11].

The size and amount of added aluminum was optimized via evaluation of various reinforced specimens that were simply fabricated using a uni-axial press instead of the tape-casting method. The mechanical strength of these specimens is plotted against heat-treatment time and aluminum content in Figs. 5 and 6, respectively. The mechanical strength generally increases up to 50 h, but then decreases with further heat-treatment. With the addition of aluminum and $Li_2CO_3$ particles to the specimens, their strength improves relative to those having a matrix reinforced only with aluminum. This is attributed to the mechanical strength being largely affected by the melting of aluminum and by the transformation to $LiAlO_2$ via the reaction of Al and $Li_2CO_3$. The optimized amount of added Al and the optimized Al size are shown in Fig. 6. All aluminum sizes display the same tendency in their curves, and give the highest mechanical strength near 4 vol.%. In addition, an increase in the size of the aluminum particles leads to a higher strength. The best results are obtained at an aluminum size and content of 50 μm and 4 vol.%, respectively.

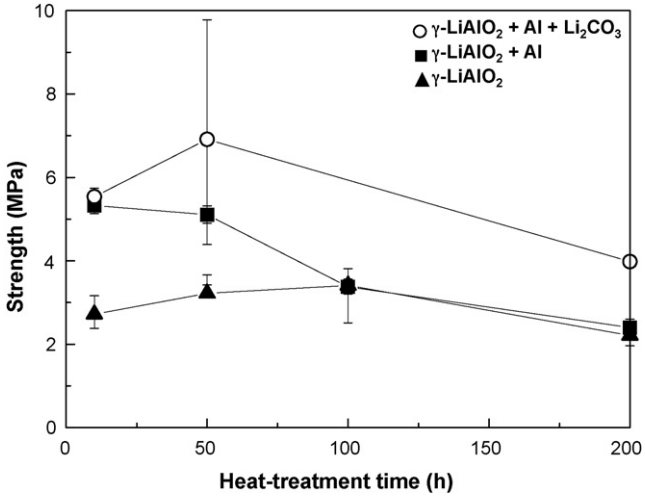


Fig. 5. Flexural strength variation of γ-$LiAlO_2$ specimens with heat-treatment time: (◯) mixture of γ-$LiAlO_2$, Al (5 vol.%) and $Li_2CO_3$; (■) mixture of γ-$LiAlO_2$ and Al (5 vol.%); (▲) pure γ-$LiAlO_2$ specimen.

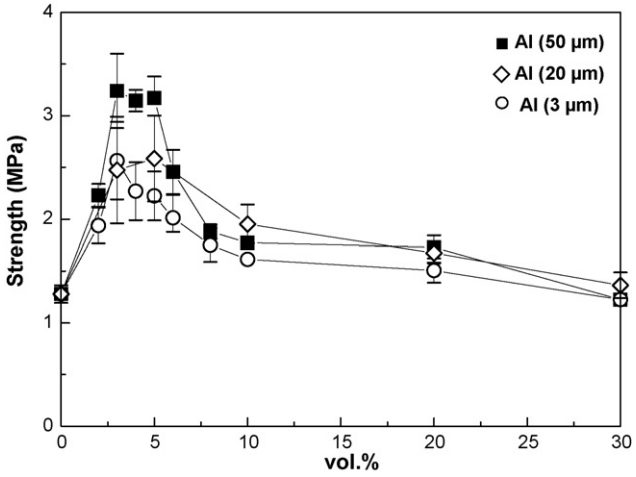


Fig. 6. Flexural strength variation of γ-$LiAlO_2$ specimens with Al vol.% reinforcement: (■) 50 μm Al; (◇) 20 μm Al; (◯) 3 μm Al.

### 3.4. Microstructures

To house the electrolyte materials ($Li/K_2CO_3$) safely between the anode and cathode electrodes, the capillary force in the matrix should be greater than that of the two electrodes. Therefore, the pore-size distribution of the matrix must be less than that of the electrodes. With respect to the pore-size distributions of the anode and cathode (3–10 μm), the pore-size distribution of the matrix generally must be 0.1–0.3 μm, i.e., 1/10th that of the two electrodes. In addition, a porosity from 50% to 70% is suitable for electrolyte retention during MCFC operation. Scanning electron micrographs of non-reinforced and aluminum-reinforced (3/20/50 μm) matrices are presented in Fig. 7. With the addition of large aluminum particles (50 μm), the large pores in the reinforced matrix surface shrink more than those in the other matrices. The aluminum-reinforced (50 μm) matrix that displays the highest strength has a porosity of 61% and a pore size of 0.1 μm, as shown in Fig. 8.

### 3.5. Performance of matrices reinforced with aluminum and $Li_2CO_3$ particles

Cracks in the matrices can be investigated by two measurement methods, evaluation of the $N_2$ gas crossover in the anode exit for the cathode oxidant gas (in the present case) and assessment of the open-circuit voltage (OCV) in a single-cell test. The $N_2$ gas measurement results are given in Fig. 9. For eight thermal cycles, the use of standard matrices results in a $N_2$ gas composition of lower than 3 vol.%. During the next stage of thermal cycles, however, the $N_2$ gas gradually increases. By contrast, Al-reinforced matrices show less than 2 vol.% of $N_2$ gas crossover up to 15 thermal cycles. The results from electrical performance tests of a single cell are presented in Fig. 10. For a standard matrix, the OCV is 1.050 V whereas the initial cell voltage at 150 mA $cm^{-2}$ is 0.87 V. After eight cycles, the OCV decreases to 1.025 V as the amount of $N_2$ gas crossover increases. The cell voltage at 150 mA $cm^{-2}$ exhibits a similar pattern. For reinforced matrices, the OCV is 1.070 V and

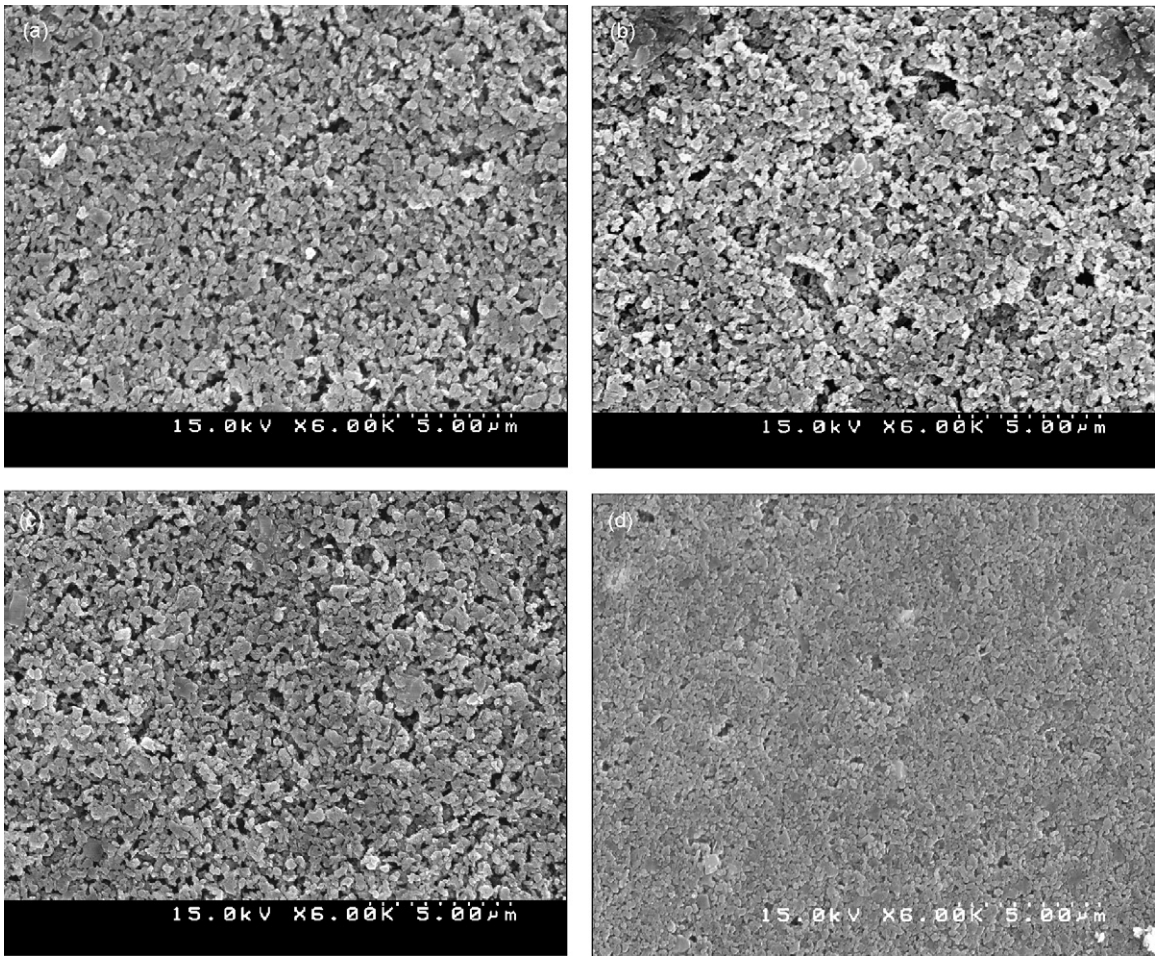


Fig. 7. Scanning electron micrographs of fracture surfaces of γ-$LiAlO_2$ matrices with various sizes of Al reinforcement: (a) standard, (b) 3 μm Al, (c) 20 μm Al, and (d) 50 μm Al.

the initial cell voltage under the given current is 0.83 V. The rod-shaped reinforced matrix shows stable results during 28 thermal-cycling tests [7]. Rod-shaped particles, however, are not easily fabricated and require a complicated process. In the case of Al-reinforced matrices, the improvement yielded by the tape-casting method is evident. Given that these matrices are stable up to the 15th thermal-cycling test, they show good prospects for application as an improved electrolyte matrix for MCFCs.

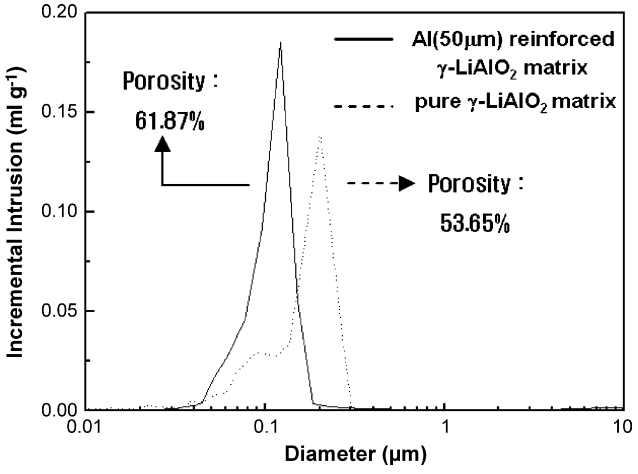


Fig. 8. Pore-size distribution of standard and 50 μm aluminum (5 vol.%)-reinforced γ-$LiAlO_2$ matrices.

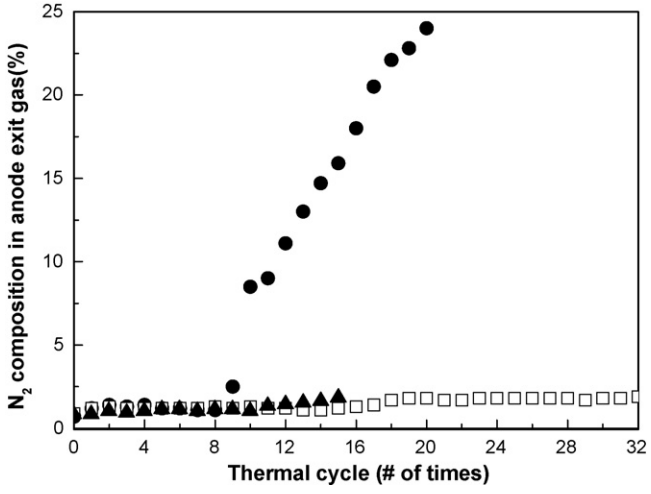


Fig. 9. $N_2$ crossover in single cell due to thermal cycling. (●) Standard γ-$LiAlO_2$ matrix; (□) rod-shaped particle reinforced matrix; (▲) 50 μm Al-reinforced γ-$LiAlO_2$ matrix.

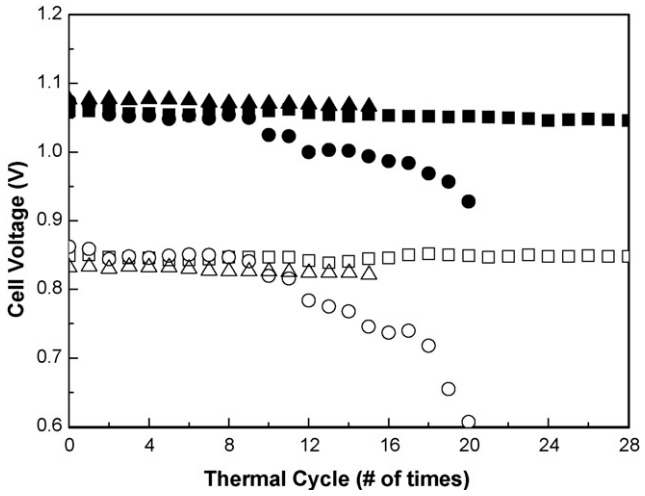


Fig. 10. Cell performances—(a) OCV: (●) standard γ-$LiAlO_2$ matrix, (■) rod-shaped particle-reinforced matrix, and (▲) 50 μm Al-reinforced γ-$LiAlO_2$ matrix; (b) current density (150 mA $cm^2$): (◯) standard γ-$LiAlO_2$ matrix, (□) rod-shaped particle-reinforced matrix, and (△) 50 μm Al-reinforced γ-$LiAlO_2$ matrix.

## 4. Conclusions

Aluminum has been examined as an economical and viable reinforcement for MCFC electrolyte matrices. The main mechanism of Al-reinforcement is found to be melting and phase transformation of the Al phase. The mechanical strength of an Al (5 vol.%) particle-reinforced MCFC matrix is increased by nearly three times in comparison with that of a γ-$LiAlO_2$ matrix by the addition of Al and $Li_2CO_3$ particles. The mismatch of the thermal expansion coefficients of the matrix and electrolyte phases can be controlled by adding Al particles. This results in an improvement in the thermal stability of the MCFC matrices in molten carbonate during the initial heating step. The performance of unit cells using an Al-reinforced γ-$LiAlO_2$ matrix is superior to that of unit cells with non-reinforced standard matrices.

## Acknowledgements

This work was supported by the Korea Electric Power Research Institute and the Korea Institute of Science and Technology Evaluation and Planning.

## References

[1] A.J. Appleby, J.R. Selman, in: H. Wendt (Ed.), Current Technology of PAFC, MCFC and SOFC Systems: Status of Present Fuel Cell Power Plants, Electrochemical Hydrogen Technologies, Elsevier, Amsterdam, 1990.
[2] A.J. Appleby, F.R. Foulkes, Fuel Cell Handbook, Van Nostrand Reinhold, New York, 1989, pp. 557–558.
[3] K. Hatoh, J. Nikura, N. Taniguchi, T. Gamo, T. Iwaki, Electrochem. Jpn. 57 (1989), pp. 728–723.
[4] Huang, Chao M., Yuh, Chao-Yi, United State Patent 5,869,203, 1999.
[5] S.-H. Hyun, S.-C. Cho, S.-A. Hong, J. Korean Ceram. Soc. 36 (1999) 107–115.
[6] S.-H. Hyun, S.-C. Cho, J.Y. Cho, D.H. Ko, J. Mater. Sci. 36 (2001) 441–450.
[7] S.-D. Kim, S.-H. Hyun, T.H. Lim, S.-A. Hong, J. Power Sources 137 (2004) 24–29.
[8] I. Lee, W. Kim, Y. Moon, H. Lim, D. Lee, J. Power Sources 101 (2001) 90–95.
[9] S.-H. Hyun, K.H. Baek, S.-A. Hong, J. Korean Ceram. Soc. 34 (3) (1997) 303.
[10] J.M. Berthelot, Composite Materials Mechanical Behavior and Structural Analysis, Springer, New York, 1996, p. 6.
[11] F.L. Matthews, R.D. Rawlings, Composite Material: Engineering and Science, Chapman & Hall, 1994, pp. 342–345.